Design of the Shift Bump Magnets for the Beam Injection of the 3-GeV RCS in J-PARC

T. Takayanagi, J. Kamiya, M. Watanabe, T. Ueno, Y. Yamazaki, Y. Irie, J. Kishiro, I. Sakai, T. Kawakubo, S. Tounosu, Y. Chida, M. Watanabe, and T. Watanuki

***Abstract*—The injection system of the 3-GeV RCS (Rapid Cycling Synchrotron) in J-PARC (Japan Proton Accelerator Research Complex) consists of four main orbit bump magnets (shift bump) to merge the injection beam with the circulating beam. In order to control the injection beam with sufficient accuracy, the shift bump magnets need a wide uniform magnetic field. The magnetic field design and the structural analysis of the shift bump magnets have been performed using three-dimensional electromagnetic and mechanical analysis codes. The shift bump magnets have realized a uniform field with less than 0.35% inhomogeneity over a wider area, which is 400 mm in width and 240 mm in height. Furthermore, the magnets operate with a high magnetic field and they are located in high radioactive level area. The flexible bar is applied to the coil as the countermeasure for thermal expansion and the insulator has strong radiation resistance.**

I. Introduction

J-PARC accelerator system consists of three accelerators: a linear accelerator (400-MeV Linac), a rapid cycling synchrotron (3-GeV RCS) [1]–[3] and 50-GeV synchrotron ring. The beam injection system of the 3-GeV RCS consists of ten bending magnets: eight horizontal bump magnets and two vertical paint magnets. The horizontal bump magnets, which are located at the long straight section in the 3-GeV RCS injection area, produce a bump orbit to merge the injection beam into the circulating beam. The horizontal bump magnets have two types: one type named "shift bump" produces a closed bump orbit and another named "paint bump" shifts the circulating beam for painting.

The machine acceptance of the shift bump is 486 π mm-mrad, and the inner size of the ceramic ducts [4] are designed to be 9 mm larger, so the beam loss can be decreased to 1 W/m. In addition, they are located in the area of the high radioactive level. The shift bump magnets have been designed for a wide good field region and to withstand levels of high radiation.

II. Parameters of the Shift Bump Magnets

The closed bump orbit is produced by the four shift bump magnets connected in series, so that the tracking of the power supply can be dispensable. The decay time of the excited current is to be less than 150 microseconds in order to protect the charge exchange foil against the excessive foil hits by the circulating beam. When the maximum exciting current of 32.2 kA is decaying, 6 kV maximum voltages are applied to the magnet against ground. The shift bump magnets have a longitudinally split structure to insert a foil for H0 beam stripping. The parameters of the shift bump magnets are shown in Table I.

TABLE I
Parameters of the Shift Bump

Parameter	Value
Number of magnets	4
Structure	W- frame
Core Length [mm]	400 - 400
Turns per Coil	2
Gap Height [mm]	310
Coil Inside Distance [mm]	616
Maximum Current [A] (400 MeV injection)	32200
Maximum Field [T]	0.2611
Maximum Magnet Voltage [kV]	6
Inductance [H] (3D calculation)	18.3×10^{-6}
Beam Stay Area [mm] (Horizontal / Vertical)	370 / 224
Lamination thickness [mm]	0.15

III. Magnet Design

The shift bump magnets have been designed using a two-dimensional electric analysis code, and three-dimensional electromagnetic and mechanical analysis codes. The schematic view of the three-dimensional model is shown in Fig. 1.

The coil of the magnets have no insulating coat. Therefore, the design of the core and the coil has to consider the breakdown by of the electric field. Furthermore, a wide good field region of the magnetic field, and the countermeasure of the heat loading due to eddy currents and the insulator of high radiation resistant are required.

A. Electric Field Calculation

The OPERA-2D analysis code is used for the electric field calculation. The result is shown in Fig. 2. It is necessary to set the electric field intensity less than 30 kV/cm, which is dielectric breakdown strength. The maximum electric field is 13.2 kV/cm for 10 kV design voltage. The shift bump magnets have a 20 mm space gap between the core and the coil and two times longer

Manuscript received September 19, 2005.

T. Takayanagi, J. Kamiya, M. Watanabe, T. Ueno, Y. Yamazaki, Y. Irie, and J. Kishiro are with the JAERI, Tokai-Mura, Naka-Gun, Ibaraki-Ken 319-1195, Japan (e-mail: tomohiro.takayanagi@j-parc.jp).

I. Sakai and T. Kawakubo are with the KEK, Tsukuba-shi, Ibaraki-Ken 305-0801, Japan.

S. Tounosu is with the Hitachi, Ltd, Power & Industrial Systems R&D Laboratory, Japan.

Y. Chida, M. Watanabe, and T. Watanuki are with the Hitachi, Ltd, Fusion and Accelerators Dept, Hitachi Works, Japan.

Digital Object Identifier 10.1109/TASC.2006.870515

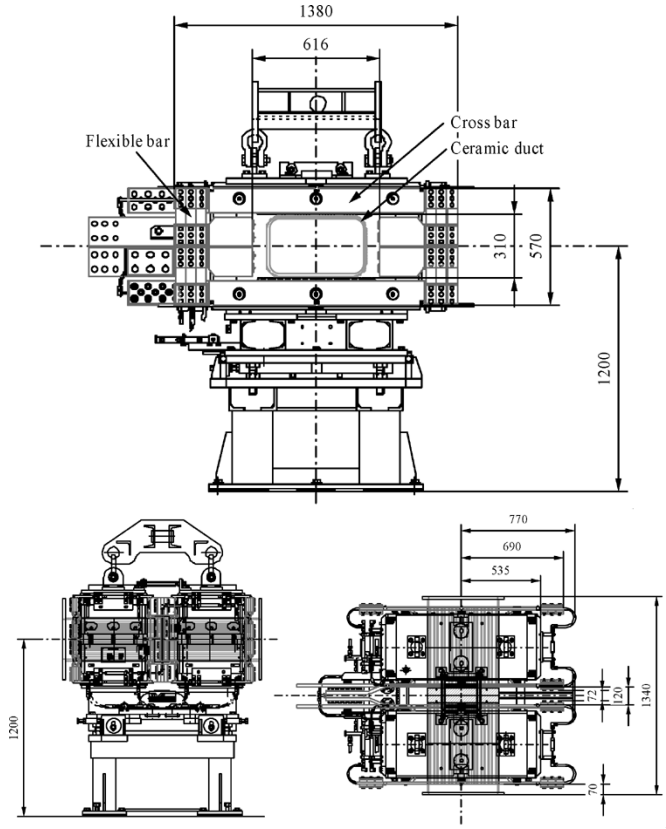

Fig. 1. Three-dimensional model of the shift bump magnet.

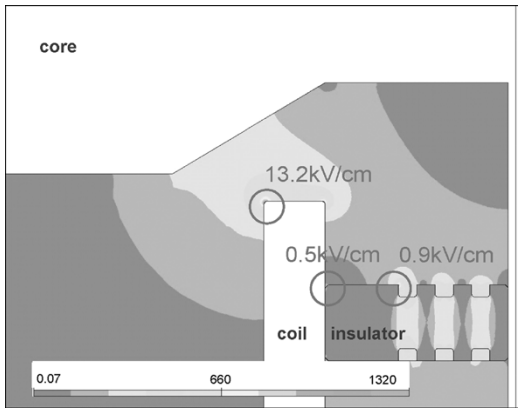

Fig. 2. Two-dimensional electric field analysis result.

distance along the coil supporting insulator than the space gap, which is the design concept to withstand a voltage of 10 kV. The 80 mm insulation distance is designed, so that the electric field intensity is very low, i.e. 0.5 kV/cm and 0.9 kV/cm.

B. Magnetic Field Calculation

The design of the core and the coil considering the magnetic field distribution is performed using three-dimensional analysis code TOSCA [5], [6]. The calculation result of the integrated magnetic field distribution is shown in Fig. 3. The area where the beam is circulating with the 486 π mm-mrad is 370 mm in width and 240 mm in height. By optimizing the coil design and the cut form of the core, a wide uniform magnetic field with less than 0.35% inhomogeneous distribution has been achieved.

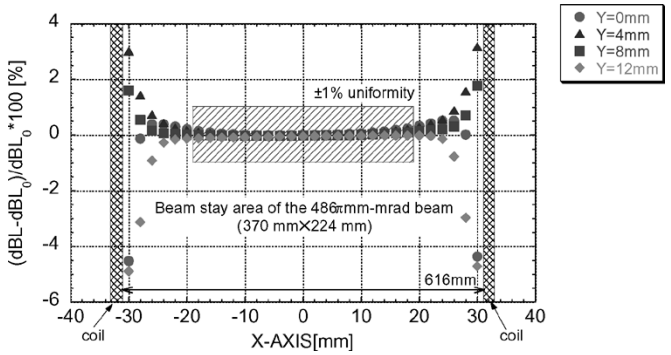

Fig. 3. Integrated magnetic field distribution of the three-dimensional analysis.

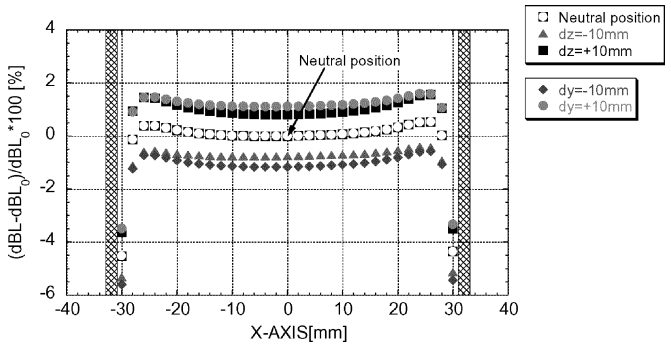

Fig. 4. Difference of the integrated magnetic field distribution by changing the position of the cross bar.

TABLE II
INDUCTANCE OF THE SHIFT BUMP

Position	Inductance [$\times 10^{-6}$H]
Neutral	1.83
dz= - 10 mm	1.87
dz= + 10 mm	1.80
dy= - 10 mm	1.79
dy= + 10 mm	1.88

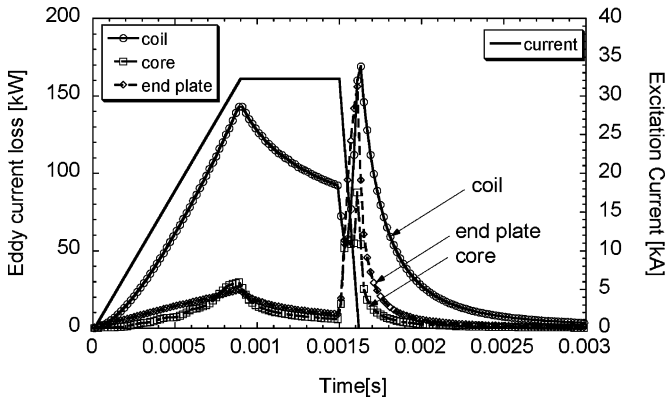

Fig. 5. Calculation result of the eddy current losses.

The shift bump magnets have high proportion of gap (310 mm) versus pole length (400 mm $\times$ 400 mm). Because of the large fringing magnetic field, the magnet inductance increase. In order to minimize the interference of the magnetic field and to prevent the high voltage of a power supply, a small

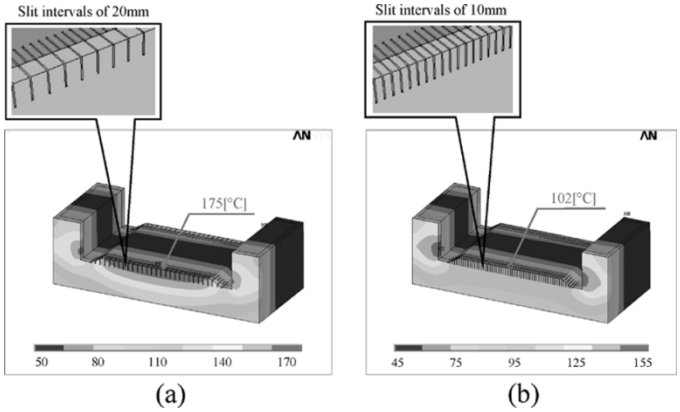

Fig. 6. Temperature of the end plate: (a) 20 mm intervals; (b) 10 mm intervals.

inductance is required. The inductance is controlled by the position of the cross bar. In case that the cross bar position is moved along the beam axis (dz) and vertically (dy), the calculation result is shown in Fig. 4. The integrated magnetic field and the distribution are changed. The distribution of the magnetic field can be optimized by changing not only the shape of the coil and the core but also the position of the cross bar. The inductance calculated by the TOSCA is given in Table II. The change of the inductance is less than 5%.

C. Eddy Current Losses

The shift bump magnets are operated at a repetition rate of 25 Hz, and are excited with a trapezoid rectangle waveform with about 1.6 milliseconds duration. Therefore, the heat loading in the core and the end plate due to the eddy current is a problem. Fig. 5 shows the calculation result of the losses using the electromagnetic field analysis code including the effects of eddy currents in three-dimension (EMSolution [7]). The highest losses are produced 0.1 milliseconds after the exciting current begins to decay at 1.5 milliseconds.

D. Slit Cut

In order to decrease the losses in the iron due to eddy currents, the magnetic core uses the laminated thin steel sheets of 0.15 mm thick [8]. The thin sheets have excellent characteristics concerning excitation loss and high-permeability. However, the end plate made of SUS 316 is 25 mm thick to withstand the pressure of lamination of 2 MPa. The end plate is provided with the slit cut in order to decrease the eddy current losses. The calculation results of the temperature, in the case of the slit intervals of 10 mm and 20 mm, respectively, are shown in Fig. 6. It is calculated using the EMSolution and the ANSYS analysis codes. Both of the end plates have slit cut that the height is 35 mm and the depth along the beam axis is 30 mm. The temperature of the end plate decreases from 175°C to 102°C by narrowing the slit intervals.

E. Coil Cooling

The temperature of the coil is also calculated using the EMSolution and the ANSYS analysis codes. The result is shown in Fig. 7. In case of no cooling, the maximum temperature of the coil is 217°C at the cross bar. The maximum temperature of the coil with cooling is 155°C and the water temperature rises by

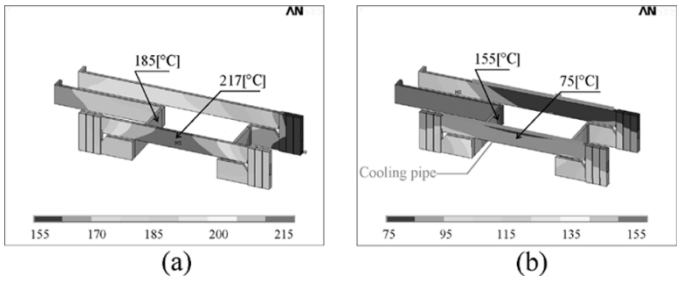

Fig. 7. Temperature of the coil: (a) without cooling; (b) with cooling.

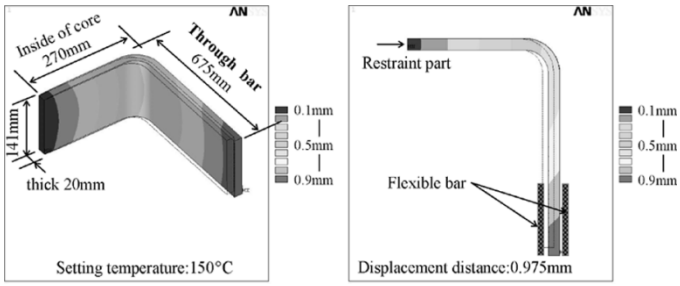

Fig. 8. Displacement due to the thermal expansion.

3°C. The cooling is only applied at the cross bar because the cooling water pipe in the magnetic pole gives the influence to the magnetic field distribution and the electric field.

F. Thermal Expansion

The maximum temperature of the coil in the magnetic pole is 155°C with cooling (Fig. 7). The cross-section of the coil is 20 mm by 141 mm. The coil displacement due to the thermal expansion is about 1 mm, as is shown in Fig. 8. It is calculated using the ANSYS analysis code [9]. In the case of 1 mm expansion, the tension of 40 tons is exerted to the cross bar and the support. Consequently, a flexible bar is applied to connect the coil with the cross bar. It is welded together at the ends of 50 cooper sheets of the 0.2 mm thick.

G. Insulator

The insulator of the coil requires a high tension and a high radiation resistance. The radiation level of 1 MGy is expected in one year in the 3-GeV RCS injection area. The machine is designed for 30 years operation. Rika Lite IGL-T (Rika-Lite) [10] is applied as the insulator supporting the coil from the core. Rika-Lite gives the good thermal endurance, chemical and the radiation resistance. Flexural strengths at 23/120/150°C (ISO 178) are 400/280/200 MPa, respectively. The ceramics, which is a famous insulator, is poor at vibratory motions due to rapid repetition effects and the thermal expanding shock. The picture of the insulator made from Rika-Lite is shown in Fig. 9. It is cut in a groove in order to produce a long insulated distance.

The test results of the resistance to temperature and radiation are shown in the Fig. 10. The test pieces are 3 mm in thickness, 10 mm in width and 80 mm in height. The test method is of the JIS K 6911. Fig. (10a) shows the dependence on the temperature without any radiation and Fig. (10b) the dependence on the radiation level at room temperature. As the temperature rises, the maximum flexural strength becomes small, and the characteristic of

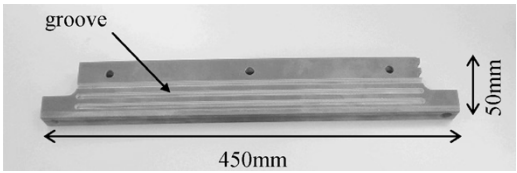

Fig. 9. Insulator of the shift bump made from a Rika-Lite.

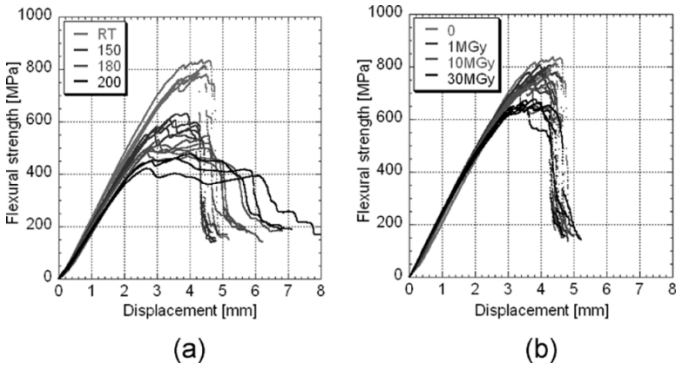

Fig. 10. Maximum flexural stress: (a) dependence on the temperature; (b) dependence on the radiation.

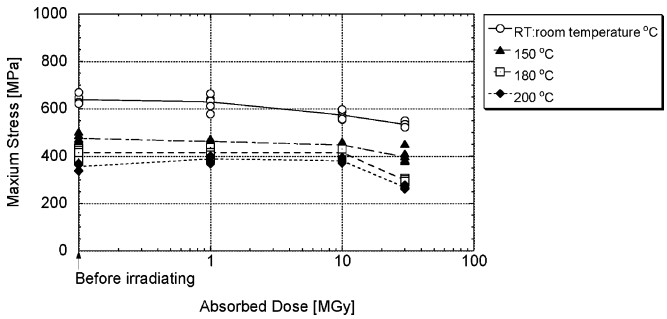

Fig. 11. Maximum flexural stress.

the flexural strength changes with displacements more than 2 mm. In contrast, the characteristic does not change with radiation.

The change of the flexural stress is plotted in Fig. 11. Although some reduction is seen with temperature, the result is satisfied as the supporting of the coil.

IV. Adjustment of the Magnetic Field

Four sets shift bump magnets are connected in series in order to form a closed bump orbit. So the total integrated magnetic field of four sets is should be zero. The analysis of the magnetic field, where the four sets of the magnets are connected in series, is calculated using the TOSCA. The calculated result is shown in Fig. 12. The total integrated magnetic field is about minus 2700 gauss-cm, which is about 0.9% of that for one set. Since the four sets of the magnets are excited by one set of a power supply, each excitation current and magnetic field can not be adjusted individually. The core of the shift bump magnets has a vertically split structure at the medium plane, and the thin insulator sheets are inserted between the cores to adjust the field balance.

The distribution of the integrated magnetic field with a 2 mm gap clearance is shown in Fig. 13. The value of the integrated magnetic field marks a 3.6% decrease. In order to cancel the negative integrated magnetic field, it is necessary to perform

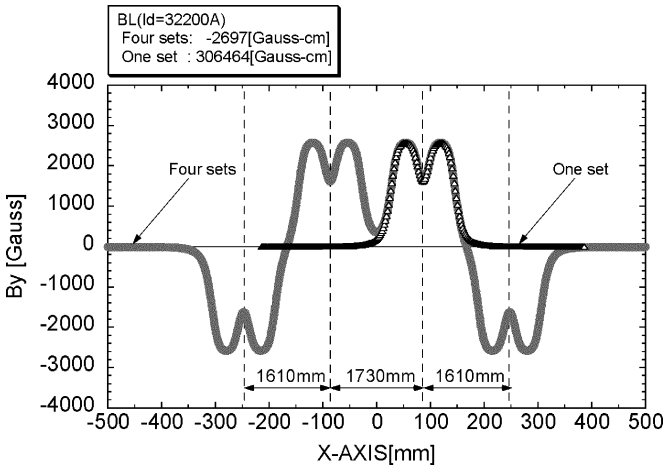

Fig. 12. Calculation result of the magnetic field of the four sets magnets are connected in series.

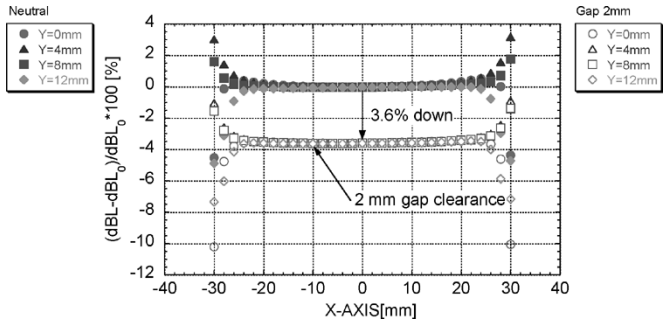

Fig. 13. Difference of the integrated magnetic field with a 2 mm gap clearance.

0.25 mm gap adjustment to the first and the fourth shift bump magnets.

V. Summary

The designs of the coil and the core of the shift bump magnets, which considered the wide magnetic field distributions and the protection of the breakdown, have been optimized using the two and three dimensional analysis codes. They have been provided with the countermeasure of the thermal expansion and the high radiation. We will have to measure the magnetic field and the temperature, and the comparison of the experimental results with the calculation results will be performed.

References

[1] Y. Irie *et al.,* in *EPAC'04*, Lucerne, July 2004, p. 113.
[2] I. Sakai *et al.,* in *PAC'03*, Portland, May 2003, p. 1512.
[3] T. Takayanagi, Y. Irie, J. Kamiya, M. Watanabe, Y. Watanabe, T. Ueno, F. Noda, P. K. Saha, T. Kawakubo, and I. Sakai, in *Proceedings of 2005 the Particle Accelerator Conference*, May 2005.
[4] M. Kinsho, T. Saito, Z. Kabeya, K. Tajiri, T. Nakamura, K. Abe, T. Nagayama, D. Nishizawa, and N. Ogiwara, "Development of alumina ceramics vacuum duct for the 3 GeV-RCS of the J-PARC project," *Vacuum*, vol. 73, pp. 187–193, 2004.
[5] Vector Fields Limited.
[6] N. Tani, T. Adachi, S. Igarashi, Y. Watanabe, H. Someya, H. Sato, and J. Kishiro, "Design of RCS magnets for J-PARC 3-GeV synchrotron," *IEEE Trans. Applied Superconductivity*, vol. 14, no. 2, pp. 409–412, June 2004.
[7] EMSolution Ver. 9.7.5, SSIL, INC..
[8] 15HTH1000, Nippon Steel Corporation.
[9] M. Kuramochi has helped with the ANSYS Ver.7 analysis..
[10] Rika-Lite Nippon Rika Kogyosho Co., Ltd..